AD-A152 690 NUMERICAL EVALUATION OF LOW FREQUENCY SOUND PROPAGATION 1/1
IN LAYERED MEDIA(U) ADMIRALTY MARINE TECHNOLOGY
ESTABLISHMENT TEDDINGTON (ENGLAND.. E A SKELTON FEB 85
UNCLASSIFIED AMTE(N)TM85015 DRIC-BR-94899 F/G 12/1 NL

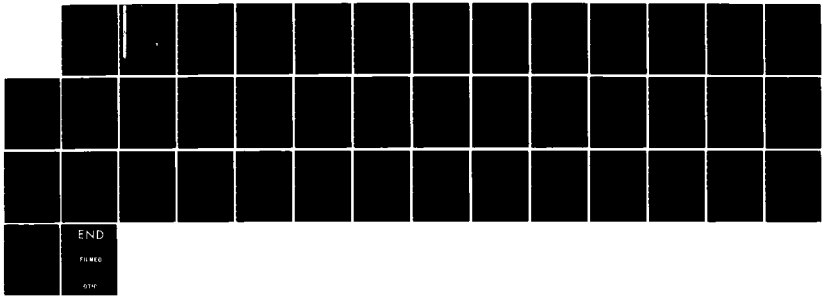

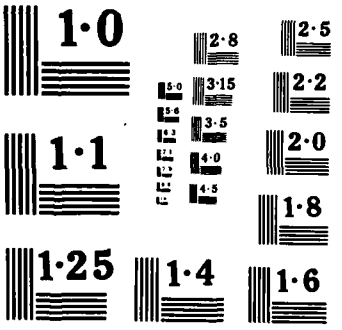
1·0
1·1
1·25
1·4
1·6
1·8
2·0
2·2
2·5
2·8
3·15
3·5
4·0
4·5
5·0

(3)

TECH MEMO AMTE(N)TM85015

COPY No. 18

AMTE(N)TM85015

ADMIRALTY RESEARCH ESTABLISHMENT (MARINE TECHNOLOGY)

NUMERICAL EVALUATION OF LOW FREQUENCY SOUND PROPAGATION IN LAYERED MEDIA

E.A. SKELTON

ARE (Teddington)
Queen's Rd TEDDINGTON
Middlesex TW11 OLN

FEBRUARY 1985

UNLIMITED

~~UNCLASSIFIED/UNLIMITED~~

AMTE(N)TM85015

NUMERICAL EVALUATION OF LOW FREQUENCY SOUND PROPAGATION IN LAYERED MEDIA

BY

E A SKELTON

Summary

A horizontally layered system of fluids and solids is bounded above and below by half-spaces which may be solid or fluid. The method of dynamic stiffness coupling is used to obtain a matrix relation connecting 'spectral' displacements and external stresses at the interfaces. The pressure due to a time-harmonic acoustic point source is obtained, via this matrix relation, by numerical evaluation of a Hankel transform; 'exactly' using a Gaussian quadrature formula and approximately using the FFT algorithm. Numerical results demonstrate that the Fortran programs are a valuable tool for predicting short-range sound propagation at low frequencies.

44 pages
11 figures

ARE(Teddington)
Queen's Road
TEDDINGTON Middlesex TW11 0LN

February 1985

C O N T E N T S

INTRODUCTION

An important and challenging research area in the field of underwater acoustics is the problem of short-range sound propagation at low frequencies. The capability to predict and understand the sound characteristics of an acoustic noise range would facilitate greatly the interpretation of the measured data which are invariably contaminated by reflections from the sea-surface and seabed; additionally, it would be a valuable research tool for studying the variety of seismic waves that may occur in a layered seabed.

The basic mathematical model used to study low-frequency propagation is the Pekeris model [1,2,3] which consists of a time-harmonic point source in a layer of fluid which is bounded above by a vacuum and bounded below by a half-space of fluid whose density and sound velocity differ from those of the fluid layer. Clement [4] has given some numerical results, obtained from a Hankel transform by numerical integration, of the Pekeris model, and has also included for comparison purposes numerical results obtained from its image approximation, which is a simple closed-form expression obtained by summing the images realized by repeated reflection in the sea surface and seabed. However, because the seabed is likely to consist of a layer of sediment overlaying a solid substrate, a propagation model in which the seabed is multilayered is desirable.

The amount of previous work on sound propagation in multi-layered media is too great to reference here. Publications by Mook et al. [5] and Schmidt & Jensen [6] contain a comprehensive list of references. In most multilayered models the acoustic field due to a time harmonic point source excitation is evaluated by numerical integration of a Fourier or Hankel transform. Mook et al., in an interesting paper on numerical aspects, demonstrate that computation is much more reliable and quicker if the poles associated with real free-waves in fluid layers can be removed from the integrand and treated explicitly: however, it is not clear that this method would be practical when elastic layers which include dissipation are considered. Schmidt & Jensen have developed an efficient method for solving numerically the sound field in a system consisting of acoustic fluid and elastic solid layers: they use the fast Fourier transform to evaluate the pressure at large distances from the source.

The approach to be used herein is the method of dynamic stiffness coupling in the 'spectral' domain which has been developed at ARE (Teddington) to analyse the sound radiation from layered media excited by time-harmonic point forces or acoustic sources [7,8,9]. The method generates a complex frequency dependent band-matrix, which relates 'spectral' excitations and displacements at the layer interfaces, from the individual dynamic stiffness matrices of the layer elements. Thus, the method has much in common with the well-known finite element method. Moreover, the matrix operations required to give the spectral displacements are usually better conditioned than those of the transfer matrix method, which is frequently used in problems of this type.

2. PROBLEM FORMULATION

(a) General

The mathematical model for a horizontally stratified ocean and seabed is shown in Figure 1. It consists of an arbitrary number of homogeneous layers whose pressures and particle displacements are solutions of the exact linearized equations of acoustics, elasto-dynamics or visco-dynamics. It is excited by a time-harmonic point source of sound which is located in one of the acoustic fluids. The time-harmonic factor $\exp(-i\omega t)$, where ω is the radian frequency, is omitted from all equations.

(b) Hankel Transforms

For the axi-symmetric problem considered here, it is convenient to represent the unknowns by Hankel transforms and their inverses, viz.,

$$\begin{bmatrix} u_r(r,z) \\ u_z(r,z) \\ p(r,z) \end{bmatrix} = (1/2\pi) \int_0^\infty \begin{bmatrix} J_1(\alpha r)\bar{u}_r(\alpha,z) \\ J_0(\alpha r)\bar{u}_z(\alpha,z) \\ J_0(\alpha r)\bar{p}(\alpha,z) \end{bmatrix} \alpha d\alpha \qquad (2.1)$$

$$\begin{bmatrix} \bar{u}_r(\alpha,z) \\ \bar{u}_z(\alpha,z) \\ \bar{p}(\alpha,z) \end{bmatrix} = 2\pi \int_0^\infty \begin{bmatrix} J_1(\alpha r)u_r(r,z) \\ J_0(\alpha r)u_z(r,z) \\ J_0(\alpha r)p(r,z) \end{bmatrix} r dr \qquad (2.2)$$

In the above equations u_r and u_z are the radial and vertical components of the particle displacement, and p is the acoustic pressure.

(c) System Matrix Equation

The spectral dynamic stiffness matrices of the various components of the system relate 'spectral' stresses or pressures to 'spectral' displacements at the component's interface(s). The matrices

$$\underset{2*2}{[\bar{S}_P(\alpha)]}, \quad \underset{4*4}{[\bar{S}_E(\alpha)]}, \quad \underset{4*4}{[\bar{S}_V(\alpha)]} \qquad (2.3)$$

for the acoustic, elastic and viscous layers, respectively, are obtained in Sections 3-5. The matrices for the upper (U) and lower (L) half-spaces,

$$\underset{1*1}{[\bar{S}_P^U(\alpha)]}, \quad \underset{2*2}{[\bar{S}_E^U(\alpha)]}, \quad \underset{2*2}{[\bar{S}_V^U(\alpha)]} \qquad (2.4a)$$

$$[\bar{S}^L_P(\alpha)],\ [\bar{S}^L_E(\alpha)],\ [\bar{S}^L_V(\alpha)] \qquad (2.4b)$$
$$1*1 \qquad 2*2 \qquad 2*2$$

are obtained in Section 6.

The assembly of these component matrices to form the system dynamic stiffness matrix relation

$$[SM(\alpha)]\ [\bar{U}(\alpha)] = [EM(\alpha)] \qquad (2.5)$$
$$M*M \qquad M*1 \qquad M*1$$

where $M=2N+2$ with N being the number of layers, is a standard procedure in finite element theory which reflects continuity of displacement and equilibrium of stress at the interfaces. It is discussed in Section 9. The matrix $[SM(\alpha)]$ is the system dynamic stiffness matrix whose elements are (in general) complex and whose bandwidth is 7.

In equation (2.5) the matrix $[EM(\alpha)]$ is a column vector of externally applied spectral forces, at the interfaces, which are due to the time-harmonic point source excitation. Externally applied stresses are defined to be positive when acting in the positive direction of the coordinate axes, see Figure 2. This matrix is derived in Section 7 for the cases in which the source is either in an acoustic layer or in an acoustic half-space.

The spectral displacements at the $N+1$ interfaces

$$[\bar{U}(\alpha)] = [\bar{U}_{r1}(\alpha),\bar{U}_{z1}(\alpha),\ldots,\bar{U}_{r(N+1)}(\alpha),\bar{U}_{z(N+1)}(\alpha)]^T \qquad (2.6)$$

are found by matrix inversion of equation (2.5). In Section 8 the pressure in an acoustic layer or half-space is obtained from knowledge of $[\bar{U}(\alpha)]$.

3. ACOUSTIC FLUID LAYER

(a) General

Figure 2A shows a section through an acoustic fluid layer with lower boundary at $z=0$ and upper boundary at $z=h$. These surfaces are subject to prescribed normal 'spectral' pressures

$$[\bar{p}(\alpha)] = [\bar{p}(\alpha,h),\bar{p}(\alpha,0)]^T \qquad (3.1)$$

which produce, normal to the surfaces, the 'spectral' displacements

$$[\bar{u}_z(\alpha)] = [\bar{u}_z(\alpha,h),\bar{u}_z(\alpha,0)]^T \qquad (3.2)$$

A matrix $[\bar{S}_p(\alpha)]$ is required which relates the 'spectral'

pressures and displacements by the relation

$$\underset{2*2}{[\bar{S}_p(\alpha)]}\underset{2*1}{[\bar{u}_z(\alpha)]} = \underset{2*1}{[\bar{p}(\alpha)]} \tag{3.3}$$

(b) Equations of Motion

The spectral solution of the linearized wave equation

$$\nabla^2 p(r,z) + k^2 p(r,z) = 0 \tag{3.4}$$

is obtained via the Hankel transform, equation (2.1), as

$$\bar{p}(\alpha,z) = A_1(\alpha)\exp(i\gamma_F z) + A_2(\alpha)\exp(-i\gamma_F z) \tag{3.5}$$

where $\gamma_F = (k^2-\alpha^2)^{1/2}$ with $\mathrm{Im}(\gamma_F)\geq 0$ in order to satisfy the radiation condition; $k=\omega/c$ is the acoustic wavenumber; ω is the radian frequency and c is the sound velocity of the fluid whose density is ρ.

Equation (3.5) and the acoustic momentum equation

$$\partial\bar{p}(\alpha,z)/\partial z = \rho\omega^2\bar{u}_z(\alpha,z) \tag{3.6}$$

evaluated at the layer boundaries gives the matrix equation

$$\begin{bmatrix}\bar{p}(\alpha,h)\\ \bar{p}(\alpha,0)\end{bmatrix} = \begin{bmatrix}\exp(i\gamma_F h) & \exp(-i\gamma_F h)\\ 1 & 1\end{bmatrix}\begin{bmatrix}A_1(\alpha)\\ A_2(\alpha)\end{bmatrix} \tag{3.7}$$

and

$$\begin{bmatrix}\bar{u}_z(\alpha,h)\\ \bar{u}_z(\alpha,0)\end{bmatrix} = (i\gamma_F/\rho\omega^2)\begin{bmatrix}\exp(i\gamma_F h) & -\exp(-i\gamma_F h)\\ 1 & -1\end{bmatrix}\begin{bmatrix}A_1(\alpha)\\ A_2(\alpha)\end{bmatrix} \tag{3.8}$$

from which $[A_1(\alpha),A_2(\alpha)]^T$ may be eliminated to give the matrix equation (3.3) as

$$(\rho\omega^2/\gamma_F\sin\gamma_F h)\begin{bmatrix}-\cos\gamma_F h & 1\\ -1 & \cos\gamma_F h\end{bmatrix}\begin{bmatrix}\bar{u}_z(\alpha,h)\\ \bar{u}_z(\alpha,0)\end{bmatrix} = \begin{bmatrix}\bar{p}(\alpha,h)\\ \bar{p}(\alpha,0)\end{bmatrix} \tag{3.9}$$

4. ELASTIC LAYER

(a) General

Figure 3A shows a section through an elastic layer with lower boundary at $z=0$ and upper boundary at $z=h$. These surfaces are subject to prescribed tangential and normal 'spectral' stresses

$$[\bar{\tau}(\alpha)] = [\bar{\tau}_{rz}(\alpha,h), \bar{\tau}_{zz}(\alpha,h), \bar{\tau}_{rz}(\alpha,0), \bar{\tau}_{zz}(\alpha,0)]^T \qquad (4.1)$$

which produce tangential and normal 'spectral' displacements

$$[\bar{u}(\alpha)] = [\bar{u}_r(\alpha,h), \bar{u}_z(\alpha,h), \bar{u}_r(\alpha,0), \bar{u}_z(\alpha,0)]^T \qquad (4.2)$$

A matrix $[\bar{S}_E(\alpha)]$ is required which relates the 'spectral' stresses and displacements by the relation

$$\underset{4*4}{[\bar{S}_E(\alpha)]}\,\underset{4*1}{[\bar{u}(\alpha)]} = \underset{4*1}{[\bar{\tau}(\alpha)]} \qquad (4.3)$$

(b) Equations of Motion

The linear elastic equation of motion [10]

$$(\lambda+\mu)\nabla(\nabla.\underline{u}) + \mu\nabla^2\underline{u} = \rho\partial^2\underline{u}/\partial t^2 \qquad (4.4)$$

may be reduced to the two wave equations

$$\begin{aligned} \nabla^2 F(r,z) + k_L^2 F(r,z) &= 0 \\ \nabla^2 G(r,z) + k_T^2 G(r,z) &= 0 \end{aligned} \qquad (4.5)$$

by means of the substitutions

$$\begin{aligned} u_r(r,z) &= \partial F(r,z)/\partial r + \partial^2 G(r,z)/\partial r\partial z \\ u_z(r,z) &= \partial F(r,z)/\partial z - \partial^2 G(r,z)/\partial r^2 - (1/r)\partial G(r,z)/\partial r \\ u_\theta &= 0 \end{aligned} \qquad (4.6)$$

The 'spectral' solutions of these wave equations are obtained via the zero order Hankel transform, equation (2.1), as

$$\bar{F}(\alpha,z) = A_1(\alpha)\exp(i\gamma_L z) + A_2(\alpha)\exp(-i\gamma_L z)$$

$$\bar{G}(\alpha,z) = A_3(\alpha)\exp(i\gamma_T z) + A_4(\alpha)\exp(-i\gamma_T z) \tag{4.7}$$

In the above equations λ and μ are the Lamé constants of he elastic material whose density is ρ; k_L is the wavenumber f longitudinal waves in the elastic solid; k_T is the wavenumber f shear waves in the elastic solid;

$$k_L = \omega/c_L = \omega/[(\lambda+2\mu)/\rho]^{1/2}$$
$$k_T = \omega/c_T = \omega/(\mu/\rho)^{1/2} \tag{4.8}$$

here c_L and c_T are respectively the velocities of ongitudinal and shear waves; $\gamma_L^2=(k_L^2-\alpha^2)^{1/2}$ and $\gamma_T^2=(k_T^2-\alpha^2)^{1/2}$, ith $Im(\gamma_L)\geq 0$ and $Im(\gamma_T)\geq 0$ in order to satisfy the radiation onditions.

c) Spectral Displacements

The 'spectral' displacements are obtained by substituting he Hankel transform representations of F and G into quations (4.6), and noting the Bessel function identities

$$x^2 d^2J_n(x)/dx^2 + x dJ_n(x)/dx + (x^2-n^2)J_n(x) = 0 \tag{4.9}$$

nd

$$dJ_0(x)/dx = -J_1(x) \tag{4.10}$$

hey are

$$\bar{u}_r(\alpha,z) = -\alpha\bar{F} - \alpha\partial\bar{G}/\partial z$$
$$\bar{u}_z(\alpha,z) = \partial\bar{F}/\partial z + \alpha^2\bar{G} \tag{4.11}$$
$$\bar{u}_\theta(\alpha,z) = 0$$

$\bar{F}$ and $\bar{G}$ may be eliminated from equations (4.11) by the use of quations (4.7) to give

$$\bar{u}_r(\alpha,z) = -\alpha A_1(\alpha)\exp(i\gamma_L z) - \alpha A_2(\alpha)\exp(-i\gamma_L z)$$
$$- i\alpha\gamma_T A_3(\alpha)\exp(i\gamma_T z) + i\alpha\gamma_T A_4(\alpha)\exp(-i\gamma_T z) \tag{4.12}$$

$$\bar{u}_z(\alpha,z) = i\gamma_L A_1(\alpha)\exp(i\gamma_L z) - i\gamma_L A_2(\alpha)\exp(-i\gamma_L z)$$

$$+ \alpha^2 A_3(\alpha)\exp(i\gamma_T z) + \alpha^2 A_4(\alpha)\exp(-i\gamma_T z)$$

(d) Spectral Stresses

It is straightforward to show that the stresses

$$\tau_{rz} = \mu(\partial u_r/\partial z + \partial u_z/\partial r)$$

$$\tau_{zz} = \lambda(\partial u_r/\partial r + u_r/r + \partial u_z/\partial z) + 2\mu\partial u_z/\partial z \qquad (4.13)$$

have the following 'spectral' representations in terms of the unknowns A_1 to A_4.

$$\bar{\tau}_{rz} = -2i\alpha\mu\gamma_L A_1(\alpha)\exp(i\gamma_L z) + 2i\alpha\mu\gamma_L A_2(\alpha)\exp(-i\gamma_L z)$$

$$+ \mu\alpha(\gamma_T^2-\alpha^2)A_3(\alpha)\exp(i\gamma_T z) + \mu\alpha(\gamma_T^2-\alpha^2)A_4(\alpha)\exp(-i\gamma_T z) \qquad (4.14)$$

$$\bar{\tau}_{zz} = -(\lambda k_L^2+2\mu\gamma_L^2)A_1(\alpha)\exp(i\gamma_L z) - (\lambda k_L^2+2\mu\gamma_L^2)A_2(\alpha)\exp(-i\gamma_L z)$$

$$+ 2i\alpha^2\mu\gamma_T A_3(\alpha)\exp(i\gamma_T z) - 2i\alpha^2\mu\gamma_T A_4(\alpha)\exp(-i\gamma_T z)$$

(e) Matrix Equation

Equations (4.12) and (4.14), evaluated at $z=h$ and $z=0$, give the matrix equations

$$\underset{4*4}{[R_E(\alpha)]}\ \underset{4*1}{[A(\alpha)]} = \underset{4*1}{[\bar{u}(\alpha)]}$$

$$\underset{4*4}{[P_E(\alpha)]}\ \underset{4*1}{[A(\alpha)]} = \underset{4*1}{[\bar{\tau}(\alpha)]} \qquad (4.15)$$

from which $[A(\alpha)]$ may be eliminated to give the required relation between surface 'spectral' stresses and displacements, viz.,

$$\underset{4*4}{[P_E(\alpha)]}\ \underset{4*4}{[R_E(\alpha)]^{-1}}\ \underset{4*1}{[\bar{u}(\alpha)]} = \underset{4*1}{[\bar{\tau}(\alpha)]} \qquad (4.16)$$

The elements of the matrices $[P_E(\alpha)]$ and $[R_E(\alpha)]$ are listed the Appendix.

VISCOUS FLUID LAYER

General

Figure 3A shows a section through a viscous fluid layer with
ver boundary at z=0 and upper boundary at z=h. The surfaces
e subject to prescribed tangential and normal 'spectral'
resses $[\bar{\tau}(\alpha)]$ which produce 'spectral' surface displacements
$(\alpha)]$. A matrix $[\bar{S}_V(\alpha)]$ is required which relates the surface
pectral' stresses and displacements by the equation

$$[\bar{S}_V(\alpha)]\,[\bar{u}(\alpha)] = [\bar{\tau}(\alpha)] \qquad (5.1)$$

$$4*4 \quad 4*1 \quad 4*1$$

Equations of Motion

The linearized Navier-Stokes equations of a viscous fluid [10]

$$-\nabla p + \mu\nabla^2\dot{\underline{u}} + (\mu/3)\nabla(\nabla.\dot{\underline{u}}) = \rho\partial\dot{\underline{u}}/\partial t$$

$$\partial\rho/\partial t + \rho\nabla.\dot{\underline{u}} = 0 \qquad (5.2)$$

$$\partial\rho/\partial t = c^2\partial\rho/\partial t$$

y be reduced to the equations

$$\nabla^2F(r,z) + [\omega^2/(c^2-4i\omega\mu/3\rho)]F(r,z) = 0$$

$$\nabla^2G(r,z) + (i\omega\rho/\mu)G(r,z) = 0 \qquad (5.3)$$

$$p = -(i\rho c^2/\omega)(\nabla.\dot{\underline{u}})$$

means of the substitutions

$$\dot{u}_r(r,z) = \partial F(r,z)/\partial r + \partial^2G(r,z)/\partial r\partial z$$

$$(5.4)$$

$$\dot{u}_z(r,z) = \partial F(r,z)/\partial z - \partial^2G(r,z)/\partial r^2 - (1/r)\partial G(r,z)/\partial r$$

In the above equations μ is the dynamic coefficient of
scosity of the fluid whose density is ρ, and in which the
und speed is c. The overdot $(\dot{})$ denotes differentiation
th respect to time.

Equations (5.3) and (5.4) together with the stress-velocity
lations

$$\tau_{rz} = \mu(\partial\dot{u}_r/\partial z + \partial\dot{u}_z/\partial r) \qquad (5.5)$$

C the sound levels exceed the datum. The plots are consistent
h two free-waves in the water whose amplitudes decrease with
tance from the free-surface and the sediment interface,
pectively.

The situation is more complex at 5, 7 and 9Hz, shown in
ures 7-9. Here the increasing number of wavenumber branches
es physical interpretation difficult without the availability
eigenvectors. The most interesting feature in these plots is
short-wavelength interference pattern obtained when both the
rce and hydrophone are near to the bottom: this is due to the
eraction between the short-wavelength free-wave which is
dominantly a shear wave in the sediment (labelled 1 in Figure
, and the other waves whose wavelengths are much larger.

Effect of Shear

Figures 10 and 11 show the sound level versus distance plots
ained by Gaussian integration when the sediment layer and
er half-space are both treated as acoustic fluids. The
quencies chosen for these plots were 5 and 9Hz, respectively.
omparison of Figures 7 and 10, which are plots for 5Hz, shows
t the effect of shear is strongest when both the source and
receiver are near to the bottom: as expected, the short-
elength interference effect disappears when shear is omitted.
omparison of Figures 9 and 11, which are plots for 9Hz, shows
or differences at all three source/receiver positions, the
t striking being in the case in which both source and receiver
near to the bottom.

Sound Levels by FFT Integration

The fast Fourier transform algorithm has also been used to
luate the Hankel transform. Plots corresponding to those in
ures 5-9 have been obtained but they are not reproduced here
ause they are almost indistinguishable from those obtained by
ssian quadrature at 3, 5, 7 and 9Hz; and at 1Hz they differ by
to 3dB - which result is not surprising because the FFT
ults are strictly valid only when $kr>1$.

The Gaussian method was found to be more efficient than the
method because whereas the former requires a high sampling
sity of the integrand only near to free-wavenumbers, the
ter requires a high (equally spaced) sampling density through-
the range of integration. One of the disadvantages of the
ssian method is the large number of Bessel function evaluat-
s required, but this could be somewhat alleviated by inter-
ation or computations of restricted accuracy. A subsequent
lication will give a detailed comparison of numerical results
ained by the two methods, and will also discuss the parameters
essary for numerical integration.

propagating free-waves to exist, the values of γ_L and γ_T in the underlying elastic half-space must be purely imaginary. Thus, the real wavenumbers of free-waves are constrained to lie in the region

$$\alpha > k_T(\text{rock}) > k_L(\text{rock}) \qquad (11.1)$$

and the wave amplitudes in the lower half-space must decay exponentially with distance from the interface.

Each branch of the dispersion plot represents free-waves which are various combinations of longitudinal waves in the water layer and shear and longitudinal waves in the sediment layer and rock half-space. The relative magnitudes of these waves may be determined exactly by calculating the eigenvectors of the matrix $[SM(\alpha)]$ for each pair of values of α and ω, but some general speculations are possible without doing so.

As the frequency is increased the character of each free-wave changes. The branch labelled 1 starts as a coupled wave whose motion is predominantly longitudinal in the sediment layer and rock half-space, it then changes rapidly to a predominantly shear wave in the sediment. The branches labelled 2 and 3 start as predominantly longitudinal waves in the sediment, turn into acoustic waves in the fluid, and then later change into predominantly shear waves in the sediment. The branch labelled 4 starts as a longitudinal wave in the sediment and turns into a shear wave in the sediment. The branch labelled 5 starts as predominantly a shear wave in the sediment and turns into a longitudinal wave in the sediment.

Figure 4B shows the real branches of the radial wavenumber versus frequency plot for the system in which shear is absent in the sediment layer and rock half-space, i.e. they are both treated as fluids. The wavenumbers are constrained to lie in the region

$$\alpha > k(\text{rock}) \qquad (11.2)$$

and they are not too dissimilar from the wavenumbers that would have been obtained in the absence of the fluid sediment layer. A comparison of Figures 4A and 4B shows that shear plays a significant role in determining the wavebearing properties of the system.

(c) Sound Levels by Gaussian Integration

Figures 5-9 show the sound level versus distance plots obtained by Gaussian integration for the three (A,B,C) source/receiver positions. At 1Hz, shown in Figure 5, the sound level decreases rapidly with distance but tends to level off when the hydrophone is located on the bottom. This is consistent with the presence of a coupled free-wave in the sediment layer and rock half-space, which has only a weak component in the water layer.

At 3Hz, shown in Figure 6, the sound levels in Plot A are much less than those of the spherical spreading datum: in Plots B

. NUMERICAL RESULTS

) General

The material and geometric constants in SI units, used in e computation of sound propagation, in a layer of water on a abed consisting of a layer of sediment on top of a hard sub- ratum, were chosen as follows:

per Half-Space:	vacuum			
yer of Water:	ρ=1000	c=1500	h=225	
yer of Sediment:	ρ=1400	$c=c_L$=1750	c_T=250	h=20
	$\lambda=4.11\times10^9$	$\mu=8.75\times10^7$		
wer Half-Space:	ρ=2500	$c=c_L$=5000	c_T=2500	
Rock)	$\lambda=3.13\times10^{10}$	$\mu=1.56\times10^{10}$		

Distance off Seabed	Plot A	Plot B	Plot C
Source	125	125	10
Hydrophone	100	1	1

us in the 'A' plot of Figures 5-11 both source and hydrophone re near to midwater; in the 'B' plot the source is near midwater nd the hydrophone is near to the bottom; and in the 'C' plot oth the source and the hydrophone are near to the bottom. The mplitude of the point source was chosen as p_0=1; hence the ound levels in dB ref. 1 micropascal at the stated range can be eferred to a free-field source strength of 120dB at 1m. The ound levels are shown as the source moves along a horizontal rack ranging from x=0 (point of closest approach to hydro- hone) to x=1000m, the horizontal separation, y, between source nd hydrophone at the point of closest approach being selected as 0m. Each of the plots contains the spherically spreading case, =$20.0\log_{10}(1/R)+120$, where $R=[x^2+y^2+(z-z_0)^2]^{1/2}$, for comparative urposes. Damping was included by setting the hysteretic loss- actors to 0.01, a value which does not introduce unduly high ttenuations at the maximum range plotted. The infinite limit of ntegration in the Hankel transform was truncated to α_{max}=0.40 hich is sufficiently high to include all the free-wavenumbers. owever, due to the limited maximum number size (10^{38}) on the DP-11 computer it was necessary to subdivide the water layer nto three to prevent numerical overflow caused by the term xp($-i\gamma_F h$).

b) Wavenumber Plots

Figure 4A shows the real branches of the radial wavenumber ersus frequency plots of the dissipationless system, in which ree-waves cut-on at 0.0, 2.2, 3.5, 6.5 and 9.0Hz. For radially

Here, the real values of α such that $\mathrm{Re}(\det[SM(\alpha)])$ vanishes are found by a simple algorithm which searches for sign changes. If $\mathrm{Im}(\det[SM(\alpha)])$ is also zero for the computed value of α then the wavenumber of a free-wave has been found.

(c) Gaussian Quadrature

The infinite limit in the integral, equation (10.1), is truncated to a finite value, α_{max}, which is determined either from a wavenumber versus frequency plot or by trial and error. The integral is then evaluated by an adaptive Gaussian quadrature (order 2) scheme, which splits the range of integration into a user selected number of equal intervals each of which is repeatedly halved until a relative convergence test is satisfied by successive approximations to the integral in the interval. Large savings in computation time are possible by parallel computation at an array of r-values, due to the simplicity of the $J_0(\alpha r)$ term in relation to $\bar{p}(\alpha,z)$.

(d) Fast Fourier Transform

The integral in equation (10.2) is proportional to

$$I(r) = \int_{-\infty}^{\infty} f(\alpha)\exp(i\alpha r)d\alpha \qquad (10.4)$$

where $f(\alpha)=\alpha^{1/2}\bar{p}(\alpha,z)$. The discrete version of this equation has been given by Cooley et al. [12] in a form which is suitable for evaluation by a fast Fourier transform algorithm, viz.,

$$I(r_j) = \delta\alpha \sum_{k=0}^{N-1} p_k \exp(2\pi i jk/N)$$

$$p_k = \sum_{q=-\infty}^{\infty} f(k\delta\alpha+Nq\delta\alpha) \qquad (10.5)$$

where $N=2^M$ with integer M; $r_j=j\delta r$ for $j=0$ to $N-1$; and $\delta\alpha=2\pi/N\delta r$. For pressure evaluation the computation time is halved when the relation

$$f(-\alpha) \equiv if(\alpha) \qquad (10.6)$$

is used when equation (10.5) is evaluated. The procedure for choosing the parameters q_{max}, N, $\delta\alpha$ (and hence δr) is to be discussed elsewhere.

The reduced matrices which occur in the case of fluid layers and half-spaces, and, if $\alpha=0$, also in the case of elastic and viscous layers and half-spaces, require no special attention before assembly into the system stiffness matrix. However, a singular system matrix which contains all zeros in certain rows may be generated, in which case the relevant diagonal terms must be set to unity.

10. COMPUTER IMPLEMENTATION

(a) Programs for Acoustic Pressure

Fortran programs have been written to evaluate numerically the sound pressure level in an acoustic layer/half-space due to the presence of a time harmonic source located in an acoustic layer/half-space. One program evaluates the pressure by Gaussian quadrature of its Hankel transform representation, viz.,

$$p(r,z) = (1/2\pi) \int_0^\infty \bar{p}(\alpha,z) J_0(\alpha r) \alpha d\alpha \qquad (10.1)$$

and another program evaluates the pressure from its asymptotic expansion for large r, viz.,

$$p(r,z) \sim (1/8\pi^3 r)^{1/2} \exp(-i\pi/4) \int_{-\infty}^\infty \bar{p}(\alpha,z) \exp(i\alpha r) \alpha^{1/2} d\alpha \qquad (10.2)$$

by the use of the fast Fourier transform algorithm.

Because the transform representations are arbitrary with respect to a solution of the corresponding homogeneous problem, it is necessary to introduce damping into the problem in order to lift any singularities off the real axis, thus permitting numerical integration. This is done by setting

$$\lambda \equiv \lambda(1-i\eta_\lambda), \quad \mu \equiv \mu(1-i\eta_\mu), \quad c \equiv c(1-i\eta_c) \qquad (10.3)$$

where the η-values are the hysteretic loss-factors.

(b) Free-Wave Propagation

In order to aid the physical interpretation of numerical results a Fortran program has been written to calculate wavenumber versus frequency dispersion curves. In the absence of external sources and dissipation, the system of homogeneous equations (2.5) has a non-trivial solution if and only if $\det[SM(\alpha)]$ vanishes. For a given value of ω there will, in general, be both real and complex values of α for which the determinant vanishes. Real values of α are the wavenumbers at which free-waves propagate, cylindrically decaying as $1/r^{1/2}$. Complex values of α may represent evanescent waves whose amplitudes decrease exponentially with distance.

$$[\bar{S}_E(\alpha)] = (\rho\omega^2/\gamma_F \sin\gamma_F h) \begin{bmatrix} 0 & 0 & 0 & 0 \\ 0 & \cos\gamma_F h & 0 & -1 \\ 0 & 0 & 0 & 0 \\ 0 & 1 & 0 & -\cos\gamma_F h \end{bmatrix} \qquad (9.3)$$

(b) Upper and Lower Half-space Elements

It is also convenient, before assembly, to write the acoustic half-space matrices in the same form as the elastic and viscous half-space matrices. Thus

$$[\bar{S}^U_P(\alpha)][\bar{u}(\alpha)] = [\bar{p}(\alpha)] \qquad (9.4)$$

and

$$[\bar{S}^L_P(\alpha)][\bar{u}(\alpha)] = [\bar{p}(\alpha)] \qquad (9.5)$$

are expanded into the form

$$[\bar{S}^U_E(\alpha)][\bar{u}(\alpha)] = [\bar{\tau}(\alpha)] \qquad (9.6)$$

and

$$[\bar{S}^L_E(\alpha)][\bar{u}(\alpha)] = [\bar{\tau}(\alpha)] \qquad (9.7)$$

in which

$$[\bar{S}^U_E(\alpha)] = (i\rho\omega^2/\gamma_F) \begin{bmatrix} 0 & 0 \\ 0 & 1 \end{bmatrix} \qquad (9.8)$$

and

$$[\bar{S}^L_E(\alpha)] = (-i\rho\omega^2/\gamma_F) \begin{bmatrix} 0 & 0 \\ 0 & 1 \end{bmatrix} \qquad (9.9)$$

(c) Computer Implementation

The assembly of the component matrices to form the system dynamic stiffness relation is a standard finite element procedure which reflects the continuity of displacement and the equilibrium of stress at the component interfaces. Computer implementation is straightforward for devotees of the finite element method. The sign convention that externally applied stresses are defined to be positive when acting in the positive direction of the co-ordinate axes makes it necessary to change the sign of the elements of the last two rows of each layer matrix, $[\bar{S}_E(\alpha)]$ and $[\bar{S}_V(\alpha)]$, and to change the sign of all the elements of the upper half-space matrix, $[\bar{S}^U_E(\alpha)]$ or $[\bar{S}^U_V(\alpha)]$, before assembling the component matrices. An example of an assembled system matrix is shown elsewhere [7].

$$\bar{p}(\alpha,z) = -i(\rho\omega^2/\gamma_F)\bar{u}_z(\alpha,0)\exp(i\gamma_F z)$$

$$+ (2\pi i p_0/\gamma_F)[\exp(i\gamma_F|z-z_0|) + \exp(i\gamma_F(z+z_0))] \qquad (8.2)$$

For the case in which there is no acoustic source in the upper half-space, it is necessary only to set $p_0=0$ in equation (8.2).

(c) In Lower Half-space

The spectral displacement $\bar{u}_z(\alpha,0)$ of the boundary of the lower half-space is obtained from the dynamic stiffness relation, equation (2.5). If the lower half-space contains a source, the spectral pressure is obtained from equations (7.11) and (7.12) evaluated at $z=0$, the boundary of the half-space. Thus after some algebra,

$$\bar{p}(\alpha,z) = i(\rho\omega^2/\gamma_F)\bar{u}_z(\alpha,0)\exp(-i\gamma_F z)$$

$$+ (2\pi i p_0/\gamma_F)[\exp(i\gamma_F|z-z_0|) + \exp(-i\gamma_F(z+z_0))] \qquad (8.3)$$

For the case in which there is no acoustic source in the lower half-space, it is necessary only to set $p_0=0$ in equation (8.3).

9. ASSEMBLY OF ELEMENTS

(a) Layer

Figure 2 shows the standard sign convention for stresses and pressures. Both displacements and externally applied stresses are defined to be positive when acting in the positive direction of the coordinate axes. Note that the directions of positive stress and positive pressure are opposite.

It is convenient, before assembly, to write the acoustic layer matrices in the same form as the elastic and viscous layer matrices. Thus

$$\underset{2*2}{[\bar{S}_P(\alpha)]}\underset{2*1}{[\bar{u}(\alpha)]} = \underset{2*1}{[\bar{p}(\alpha)]} \qquad (9.1)$$

is expanded into the form of equation (4.3)

$$\underset{4*4}{[\bar{S}_E(\alpha)]}\underset{4*1}{[\bar{u}(\alpha)]} = \underset{4*1}{[\bar{\tau}(\alpha)]} \qquad (9.2)$$

in which

Evaluation of equations (7.11) and (7.12) at $z=0$, the boundary of the lower half-space, gives the relation

$$[\bar{S}_P^L(\alpha)][\bar{u}_z(\alpha)] = [\bar{p}(\alpha)] + [E_P^L(\alpha)] \qquad (7.13)$$

in which

$$[E_P^L] = -4\pi i p_0 \exp(-i\gamma_F z_0)/\gamma_F \qquad (7.14)$$

Equations (7.13) and (7.14), together with the sign convention which requires external stresses to be positive when acting in the positive direction of the coordinate axes, show that the point source in the lower half-space is equivalent to an external vertical stress of $-E_P^L$ at the boundary of the lower half-space.

8. PRESSURE IN ACOUSTIC FLUIDS

(a) In Fluid Layer

The spectral displacements, $\bar{u}_z(\alpha,h)$ and $\bar{u}_z(\alpha,0)$, of the layer boundaries are obtained from the dynamic stiffness matrix relation, equation (2.5). If the layer contains a source, the spectral pressure is obtained from equations (7.3) and (7.4) evaluated at the layer boundaries, $z=h$ and $z=0$. Thus after some considerable algebra

$$\bar{p}(\alpha,z) = (\rho\omega^2/\gamma_F \sin\gamma_F h)[\bar{u}_z(\alpha,0)\cos\gamma_F(h-z) - \bar{u}_z(\alpha,h)\cos\gamma_F z]$$

$$- (2\pi p_0/\gamma_F \sin\gamma_F h)[\cos\gamma_F(h-|z-z_0|) + \cos\gamma_F(h-z-z_0)] \qquad (8.1)$$

For the case in which there is no acoustic source in the layer, it is necessary only to set $p_0=0$ in equation (8.1).

(b) In Upper Half-space

The spectral displacement $\bar{u}_z(\alpha,0)$ of the boundary of the upper half-space is obtained from the dynamic stiffness relation, equation (2.5). If the half-space contains a source, the spectral pressure is obtained from equations (7.7) and (7.8) evaluated at $z=0$, the boundary of the half-space. Thus after some algebra

$$E_{P2} = 4\pi p_0 \cos(\gamma_F[h-z_0])/\gamma_F \sin(\gamma_F h)$$

Equations (7.5) and (7.6), together with the sign convention which requires external stresses to be positive when acting in the positive direction of the coordinate axes, show that the point source in a fluid layer is equivalent to external normal stresses of $-E_{P1}$ and E_{P2} at the upper and lower boundaries respectively.

(c) Source in Upper Fluid Half-space

The 'spectral' form of equation (7.2) in the upper half-space is obtained from equations (7.1), (7.2) and (6.1) as

$$\bar{p}(\alpha,z) = 2\pi i p_0 \exp(i\gamma_F|z-z_0|)/\gamma_F + A_1(\alpha)\exp(i\gamma_F z) \qquad (7.7)$$

and the 'spectral' form of the momentum relation is

$$\rho\omega^2 \bar{u}_z(\alpha,z) = -2\pi p_0 \mathrm{sgn}(z-z_0)\exp(i\gamma_F|z-z_0|) + i\gamma_F A_1(\alpha)\exp(i\gamma_F z) \qquad (7.8)$$

Evaluation of equations (7.7) and (7.8) at $z=0$, the boundary of the upper half-space, gives the relation

$$[\bar{S}_P^U(\alpha)][\bar{u}_z(\alpha)] = [\bar{p}(\alpha)] + [E_P^U(\alpha)] \qquad (7.9)$$

in which

$$[E_P^U] = -4\pi i p_0 \exp(i\gamma_F z_0)/\gamma_F \qquad (7.10)$$

Equations (7.9) and (7.10), together with the sign convention which requires external stresses to be positive when acting in the positive direction of the coordinate axes, show that the point source in the upper half-space is equivalent to an external vertical stress of E_P^U at the boundary of the upper half-space.

(d) Source in Lower Fluid Half-space

The 'spectral' form of equation (7.2) in the lower half-space is obtained from equations (7.1), (7.2) and (6.4) as

$$\bar{p}(\alpha,z) = 2\pi i p_0 \exp(i\gamma_F|z-z_0|)/\gamma_F + A_2(\alpha)\exp(-i\gamma_F z) \qquad (7.11)$$

and the 'spectral' form of the momentum relation is

$$\rho\omega^2 \bar{u}_z(\alpha,z) = -2\pi p_0 \mathrm{sgn}(z-z_0)\exp(i\gamma_F|z-z_0|) - i\gamma_F A_2(\alpha)\exp(-i\gamma_F z) \qquad (7.12)$$

7. EXCITATION STRESS OF POINT SOURCE

(a) Green's Function

The pressure of a point source, located in acoustic fluid at $(r,z)=(0,z_0)$, see Figure 2, is best developed via the transform of its free-space Green's function [11].

$$p_0\exp(ikR_0)/R_0 = ip_0\int_0^\infty (1/\gamma_F)J_0(\alpha r)\exp(i\gamma_F|z-z_0|)\alpha d\alpha \qquad (7.1)$$

which is augmented by a scattering term when boundaries are present. Thus the total pressure is

$$p(r,z) = p_0\exp(ikR_0)/R_0 + p_s(r,z) \qquad (7.2)$$

where $p_s(r,z)$ satisfies the homogeneous reduced wave equation (3.1). In the above p_0 is the amplitude of the point source and $R_0=[r^2+(z-z_0)^2]^{1/2}$ is the distance from the source to the observation point.

(b) Source in Fluid Layer

The 'spectral' form of equation (7.2) is obtained from equations (7.1), (7.2) and (3.5) as

$$\bar{p}(\alpha,z) = 2\pi ip_0\exp(i\gamma_F|z-z_0|)/\gamma_F + A_1(\alpha)\exp(i\gamma_F z) + A_2(\alpha)\exp(-i\gamma_F z) \qquad (7.3)$$

and the 'spectral' form of the momentum relation, equation (3.3), is

$$\rho\omega^2\bar{u}_z(\alpha,z) = -2\pi p_0\,\mathrm{sgn}(z-z_0)\exp(i\gamma_F|z-z_0|) + i\gamma_F[A_1(\alpha)\exp(i\gamma_F z) - A_2(\alpha)\exp(-i\gamma_F z)] \qquad (7.4)$$

Evaluation of equations (7.3) and (7.4) at the layer boundaries, $z=h$ and $z=0$, gives the matrix relation

$$\underset{2\star2}{[\bar{S}_p(\alpha)]}\ \underset{2\star1}{[\bar{u}_z(\alpha)]} = \underset{2\star1}{[\bar{p}(\alpha)]} + \underset{2\star1}{[E_p(\alpha)]} \qquad (7.5)$$

in which the elements of $[E_p(\alpha)]$ are

$$E_{P1} = 4\pi p_0\cos(\gamma_F z_0)/\gamma_F\sin(\gamma_F h) \qquad (7.6)$$

and

$$\bar{\tau}_{rz} = 2i\alpha\mu\gamma_L A_2(\alpha)\exp(-i\gamma_L z) + \mu\alpha(\gamma_T^2-\alpha^2)A_4(\alpha)\exp(-i\gamma_T z)$$

$$\bar{\tau}_{zz} = -(\lambda k_L^2+2\mu\gamma_L^2)A_2(\alpha)\exp(-i\gamma_L z) - 2i\alpha^2\mu\gamma_T A_4(\alpha)\exp(-i\gamma_T z) \quad (6.14)$$

Equations (6.13) and (6.14), evaluated at $z=0$, the boundary of the lower half-space give the matrix equations

$$\underset{2*2}{[R_E^L(\alpha)]}\underset{2*1}{[A(\alpha)]} = \underset{2*1}{[\bar{u}(\alpha)]}$$

$$\underset{2*2}{[P_E^L(\alpha)]}\underset{2*1}{[A(\alpha)]} = \underset{2*1}{[\bar{\tau}(\alpha)]} \quad (6.15)$$

from which $[A(\alpha)]$ may be eliminated to give the required relation between surface 'spectral' stresses and displacements, viz.,

$$\underset{2*2}{[P_E^L(\alpha)]}\underset{2*2}{[R_E^L(\alpha)]^{-1}}\underset{2*1}{[\bar{u}(\alpha)]} = \underset{2*1}{[\bar{\tau}(\alpha)]} \quad (6.16)$$

The elements of the matrices $[P_E^L(\alpha)]$ and $[R_E^L(\alpha)]$ are listed the Appendix.

(f) Viscous Half-spaces

The method of deriving the matrices $[\bar{S}_V^U(\alpha)]$ and $[\bar{S}_V^L(\alpha)]$ is the same as that described in Section 5. Equations (6.7) and (6.12), the spectral solutions of the reduced wave equations (5.3) in the upper and lower half-spaces respectively, are substituted into equations (5.4) and (5.5). Subject to the identities (5.8) the spectral dynamic stiffness matrices of the viscous half-spaces are

$$\underset{2*2}{[\bar{S}_V^U(\alpha)]} = -i\omega\underset{2*2}{[P_V^U(\alpha)]}\underset{2*2}{[R_V^U(\alpha)]^{-1}} \quad (6.17)$$

$$\underset{2*2}{[\bar{S}_V^L(\alpha)]} = -i\omega\underset{2*2}{[P_V^L(\alpha)]}\underset{2*2}{[R_V^L(\alpha)]^{-1}} \quad (6.18)$$

in the upper half-space.

$$\bar{u}_r(\alpha,z) = -\alpha A_1(\alpha)\exp(i\gamma_L z) - i\alpha\gamma_T A_3(\alpha)\exp(i\gamma_T z)$$
$$\bar{u}_z(\alpha,z) = i\gamma_L A_1(\alpha)\exp(i\gamma_L z) + \alpha^2 A_3(\alpha)\exp(i\gamma_T z) \tag{6.8}$$

and

$$\bar{\tau}_{rz} = -2i\alpha\mu\gamma_L A_1(\alpha)\exp(i\gamma_L z) + \mu\alpha(\gamma_T^2-\alpha^2)A_3(\alpha)\exp(i\gamma_T z)$$
$$\bar{\tau}_{zz} = -(\lambda k_L^2+2\mu\gamma_L^2)A_1(\alpha)\exp(i\gamma_L z) + 2i\alpha^2\mu\gamma_T A_3(\alpha)\exp(i\gamma_T z) \tag{6.9}$$

Equations (6.8) and (6.9) evaluated at $z=0$, the boundary of the upper half-space, give the matrix equations

$$\underset{2*2}{[R_E^U(\alpha)]}\underset{2*1}{[A(\alpha)]} = \underset{2*1}{[\bar{u}(\alpha)]}$$
$$\underset{2*2}{[P_E^U(\alpha)]}\underset{2*1}{[A(\alpha)]} = \underset{2*1}{[\bar{\tau}(\alpha)]} \tag{6.10}$$

from which $[A(\alpha)]$ may be eliminated to give the required *relation between surface 'spectral' stresses and displacements*, viz.,

$$\underset{2*2}{[P_E^U(\alpha)]}\underset{2*2}{[R_E^U(\alpha)]^{-1}}\underset{2*1}{[\bar{u}(\alpha)]} = \underset{2*1}{[\bar{\tau}(\alpha)]} \tag{6.11}$$

The elements of the matrices $[P_E^U(\alpha)]$ and $[R_E^U(\alpha)]$ are listed the Appendix.

(e) Elastic Lower Half-space

The spectral solutions of the reduced wave equations (4.5) representing outgoing waves in the lower half-space are

$$\bar{F}(\alpha,z) = A_2(\alpha)\exp(-i\gamma_L z)$$
$$\bar{G}(\alpha,z) = A_4(\alpha)\exp(-i\gamma_T z) \tag{6.12}$$

which, when substituted into equations (4.11) and (4.13), give the following expressions for the spectral displacements and stresses in the upper half-space.

$$\bar{u}_r(\alpha,z) = -\alpha A_2(\alpha)\exp(-i\gamma_L z) + i\alpha\gamma_T A_4(\alpha)\exp(-i\gamma_T z)$$
$$\bar{u}_z(\alpha,z) = -i\gamma_L A_2(\alpha)\exp(-i\gamma_L z) + \alpha^2 A_4(\alpha)\exp(-i\gamma_T z) \tag{6.13}$$

the spectral stresses and displacements for both upper and lower elastic and viscous half-spaces, respectively.

(b) Acoustic Fluid Upper Half-space

The spectral solution of the linearized wave equation (3.4) representing outgoing waves in the upper half-space is

$$\bar{p}(\alpha,z) = A_1(\alpha)\exp(i\gamma_F z) \tag{6.1}$$

Equation (6.1), together with the acoustic momentum equation (3.6), evaluated at the boundary of the half-space, z=0, allows the spectral pressure to be related to the spectral displacement of the boundary, viz.,

$$\underset{1*1}{[\bar{S}_p^U(\alpha)]}\underset{1*1}{[\bar{u}(\alpha)]} = \underset{1*1}{[\bar{p}(\alpha,0)]} \tag{6.2}$$

where

$$\bar{S}_p^U(\alpha) = -i\rho\omega^2/\gamma_F \tag{6.3}$$

(c) Acoustic Fluid Lower Half-space

The spectral solution of the linearized wave equation (3.4) representing outgoing waves in the lower half-space is

$$\bar{p}(\alpha,z) = A_2(\alpha)\exp(-i\gamma_F z) \tag{6.4}$$

Equation (6.4), together with the acoustic momentum equation (3.6), evaluated at the boundary of the lower half-space, z=0, allows the spectral pressure to be related to the spectral displacement of the boundary, viz.,

$$\underset{1*1}{[\bar{S}_p^L(\alpha)]}\underset{1*1}{[\bar{u}(\alpha)]} = \underset{1*1}{[\bar{p}(\alpha,0)]} \tag{6.5}$$

where

$$\bar{S}_p^L(\alpha) = i\rho\omega^2/\gamma_F \tag{6.6}$$

(d) Elastic Upper Half-space

The spectral solutions of the reduced wave equations (4.5) representing outgoing waves in the upper half-space are

$$\begin{aligned} \bar{F}(\alpha,z) &= A_1(\alpha)\exp(i\gamma_L z) \\ \bar{G}(\alpha,z) &= A_3(\alpha)\exp(i\gamma_T z) \end{aligned} \tag{6.7}$$

which, when substituted into equations (4.11) and (4.12) give the following expressions for the spectral displacements and stresses

$$\tau_{zz} = \lambda(2\partial\dot{u}_r/\partial z + \dot{u}_r/r + \partial\dot{u}_z/\partial z) + 2\mu\partial\dot{u}_z/\partial z$$

enable the analysis to proceed as in Section 4 to give the matrix relation

$$\underset{4*4}{[P_V(\alpha)]}\ \underset{4*1}{[A(\alpha)]} = \underset{4*1}{[\bar{\tau}(\alpha)]}$$

$$\underset{4*4}{[R_V(\alpha)]}\ \underset{4*1}{[A(\alpha)]} = \underset{4*1}{[\bar{\dot{u}}(\alpha)]} \qquad (5.6)$$

from which $[A(\alpha)]$ may be eliminated to give the required relation between 'spectral' stresses and displacements, viz.,

$$-i\omega\underset{4*4}{[P_V(\alpha)]}\ \underset{4*4}{[R_V(\alpha)]^{-1}}\ \underset{4*1}{[\bar{u}(\alpha)]} = \underset{4*1}{[\bar{\tau}(\alpha)]} \qquad (5.7)$$

The elements of the matrices $[P_V(\alpha)]$ and $[R_V(\alpha)]$ are the same as those of $[P_E(\alpha)]$ and $[R_E(\alpha)]$ for the elastic layer, except that

$$\gamma_L^2 \equiv \omega^2/(c^2 - 4i\omega\mu/3\rho) - \alpha^2$$

$$\gamma_T^2 \equiv (i\omega\rho/\mu) - \alpha^2 \qquad (5.8)$$

$$\lambda \equiv i\rho c^2/\omega - 2\mu/3$$

$$\mu \equiv \mu$$

6. THE UPPER AND LOWER HALF-SPACES

(a) General

Figure 2B/2C shows a section through an acoustic half-space whose boundary, $z=0$, is subject to prescribed normal 'spectral' pressure which produces a 'spectral' displacement normal to the surface. Matrices $\underset{1*1}{[\bar{S}_P^U(\alpha)]}$ and $\underset{1*1}{[\bar{S}_P^L(\alpha)]}$ are required which relate the spectral pressures and displacements in the upper and lower half-spaces. Figure 3B/3C shows a section through an elastic or viscous half-space whose boundary, $z=0$, is subject to prescribed tangential and normal 'spectral' stresses which produce tangential and normal 'spectral' displacements. Matrices $\underset{2*2}{[\bar{S}_E^U(\alpha)]}$, $\underset{2*2}{[\bar{S}_E^L(\alpha)]}$, $\underset{2*2}{[\bar{S}_V^U(\alpha)]}$ and $\underset{2*2}{[\bar{S}_V^L(\alpha)]}$ are required which relate

12. CONCLUDING REMARKS

The mathematics of acoustic propagation in layered media has been presented in a form which is not too difficult to implement on a minicomputer by programmers familiar with the finite element method. In addition to illustrating the importance of including shear in the seabed parameters, the limited number of numerical results presented here have demonstrated the capability of the Fortran program as a potentially useful tool for predicting low frequency sound propagation characteristics at short ranges.

Some additional numerical work along the following lines is proposed as follow-up projects:

(i) comparison of results obtained from various integration algorithms including those used herein. In particular, numerical problems concerned with explicit treatment of poles [5] should be investigated when both shear and dissipation are present.

(ii) numerical studies of acoustic radiation using geometric and material constants typical of acoustic measuring ranges, and the applicability of wavenumber versus frequency plots to the physical interpretation of the results.

(iii) computation of the particle displacements in both the sea and seabed, which can be done by the existing program with trivial modification. The displacements in the sea enable acoustic intensity vectors to be calculated [3], and the displacements in the sediment would facilitate the study of low frequency seismic interface waves.

Of special value would be the availability of suitable experimental data obtained from noise ranges or scale model tests, which would help to determine the range of applicability of the theoretical work contained herein.

E A Skelton (HSO)

Manuscript completed January 1985

REFERENCES

1. BREKHOVSKIKH L.M., Waves in Layered Media. Second edition, Academic Press, 1980.

2. GABRIELSON T.B., Mathematical Foundations for Normal Mode Modelling in Waveguides, Naval Air Development Center, Warminster, Pennsylvania 18974, NADC-812484-30, February 1982. AD-A111941.

3. SKELTON E.A., Short-Range Acoustic Intensity Vectors of the Pekeris Shallow Water Model, Admiralty Marine Technology Establishment, Teddington, AMTE(N)TM83065, August 1983.

4. CLEMENT E.J., Comparison of Exact and Image Solutions of the Pekeris Shallow Water Model, Admiralty Marine Technology Establishment, Teddington, AMTE(N)TM84056, May 1984.

5. MOOK D.R., FRISK G.V., OPPENHEIM A.V., A Hybrid Numerical/ Analytical Technique for the Computation of Wave Fields in Stratified Media Based on the Hankel Transform. J. Acoust. Soc. Am., 76(1), July 1984, pages 222-243.

6. SCHMIDT H., JENSEN F.B., An Efficient Numerical Solution Technique for Wave Propagation in Horizontally Stratified Ocean Environments, Saclant Research Centre, La Spezia, Italy, Memorandum SM-173, August 1984.

7. PESTELL J.L., JAMES J.H., Sound Radiation from Layered Media, Admiralty Marine Technology Establishment, Teddington, AMTE(N)TM79423, October 1979.

8. SPICER W.J., Free-Wave Propagation in and Sound Radiation By Layered Media With Flow, Admiralty Marine Technology Establishment, Teddington, AMTE(N)TM82102, December 1982.

9. SKELTON E.A., Sound Radiation from a Cylindrical Pipe Composed of Concentric Layers of Fluids and Elastic Solids, Admiralty Marine Technology Establishment, Teddington, AMTE(N)TM83007, January 1983.

10. HUNTER S.C., Mechanics of Continuous Media, Ellis Horwood, 1976.

11. SKELTON E.A., Free-Space Green's Functions of the Reduced Wave Equation, Admiralty Marine Technology Establishment, Teddington, AMTE(N)TM82073, September 1982.

12. COOLEY J.W., et al., The Fast Fourier Transform Algorithm: Programming Considerations in the Calculation of Sine, Cosine and Laplace Transforms, J. Sound. Vib., 12(3), 1970, pages 315-337.

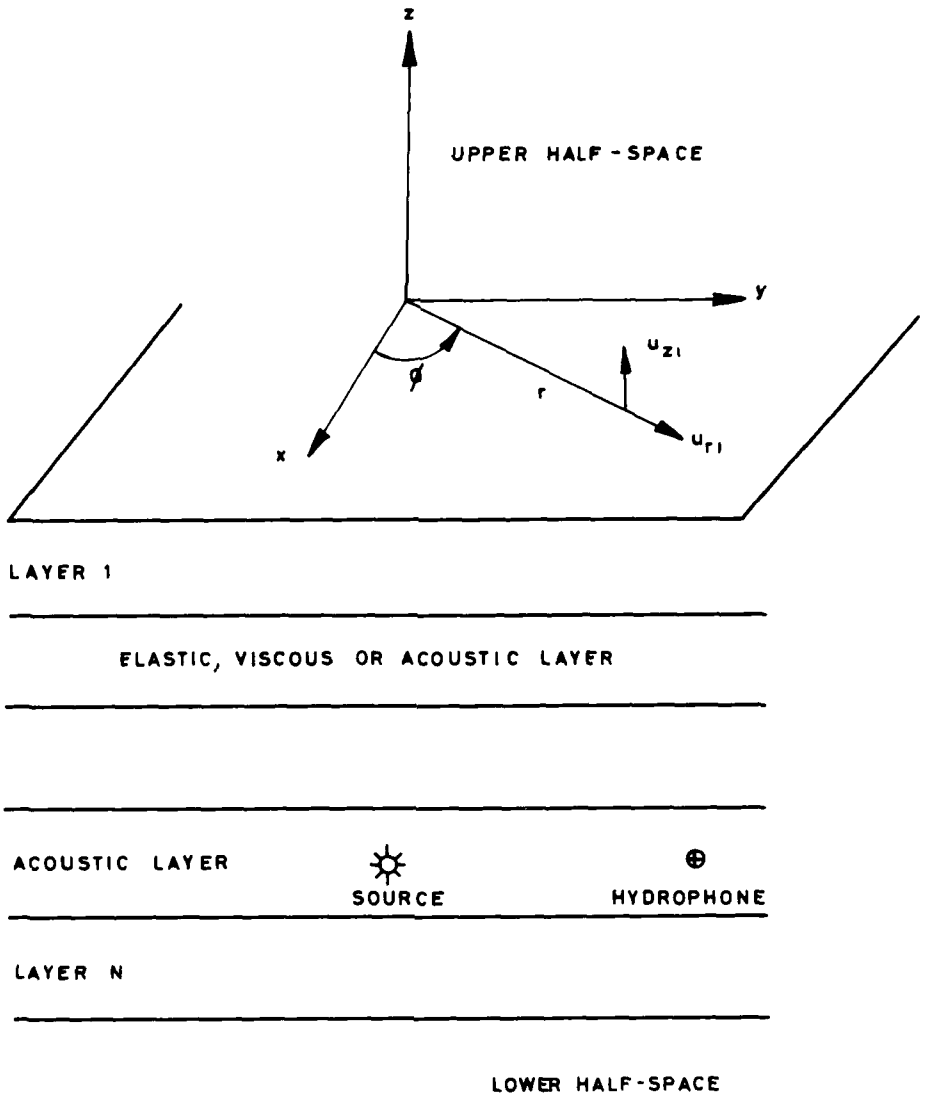

FIG. 1 MULTILAYERED SOUND PROPAGATION MODEL

3L

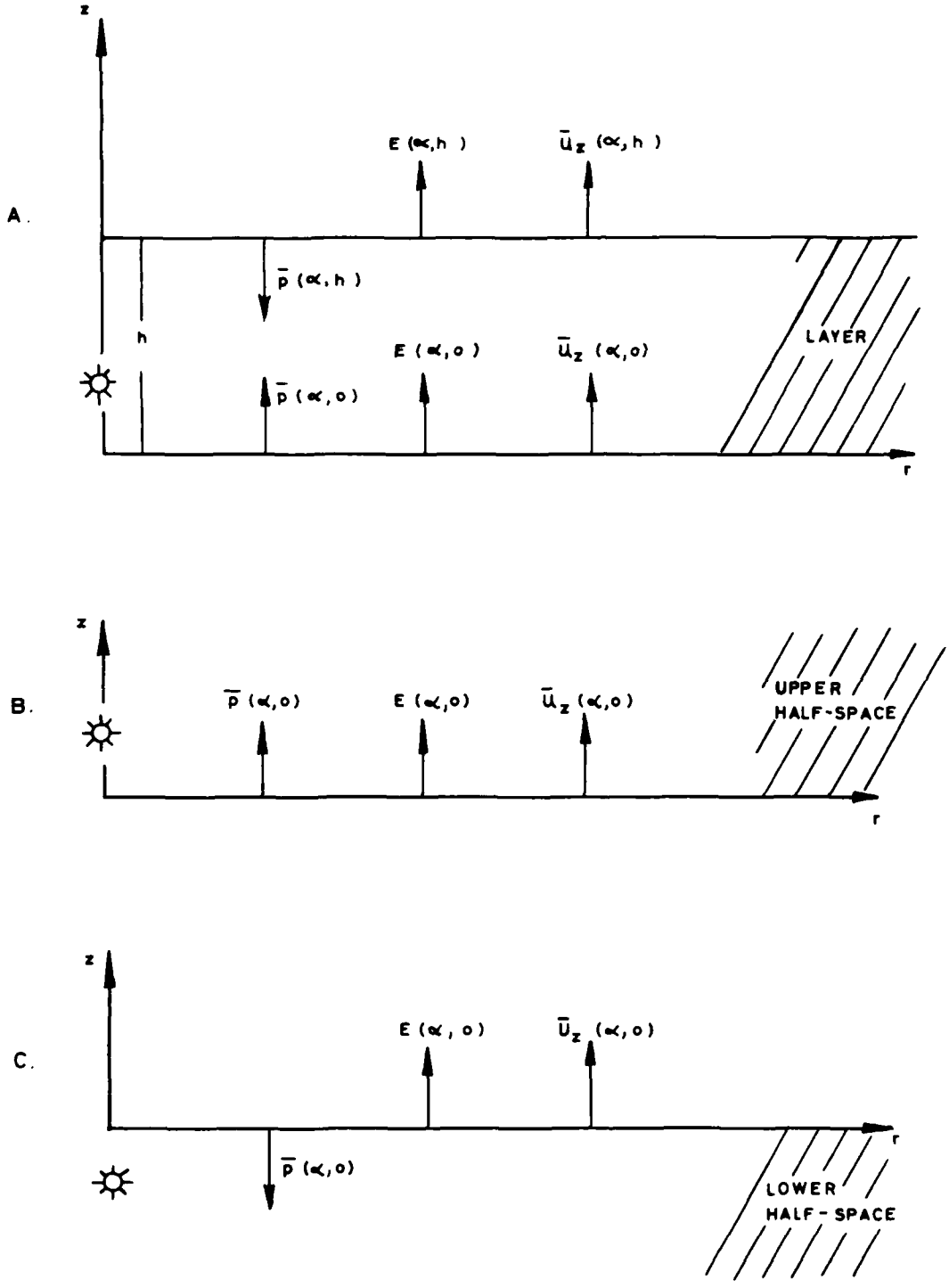

FIG. 2 SPECTRAL STRESSES AND DISPLACEMENTS OF ACOUSTIC FLUID ELEMENTS

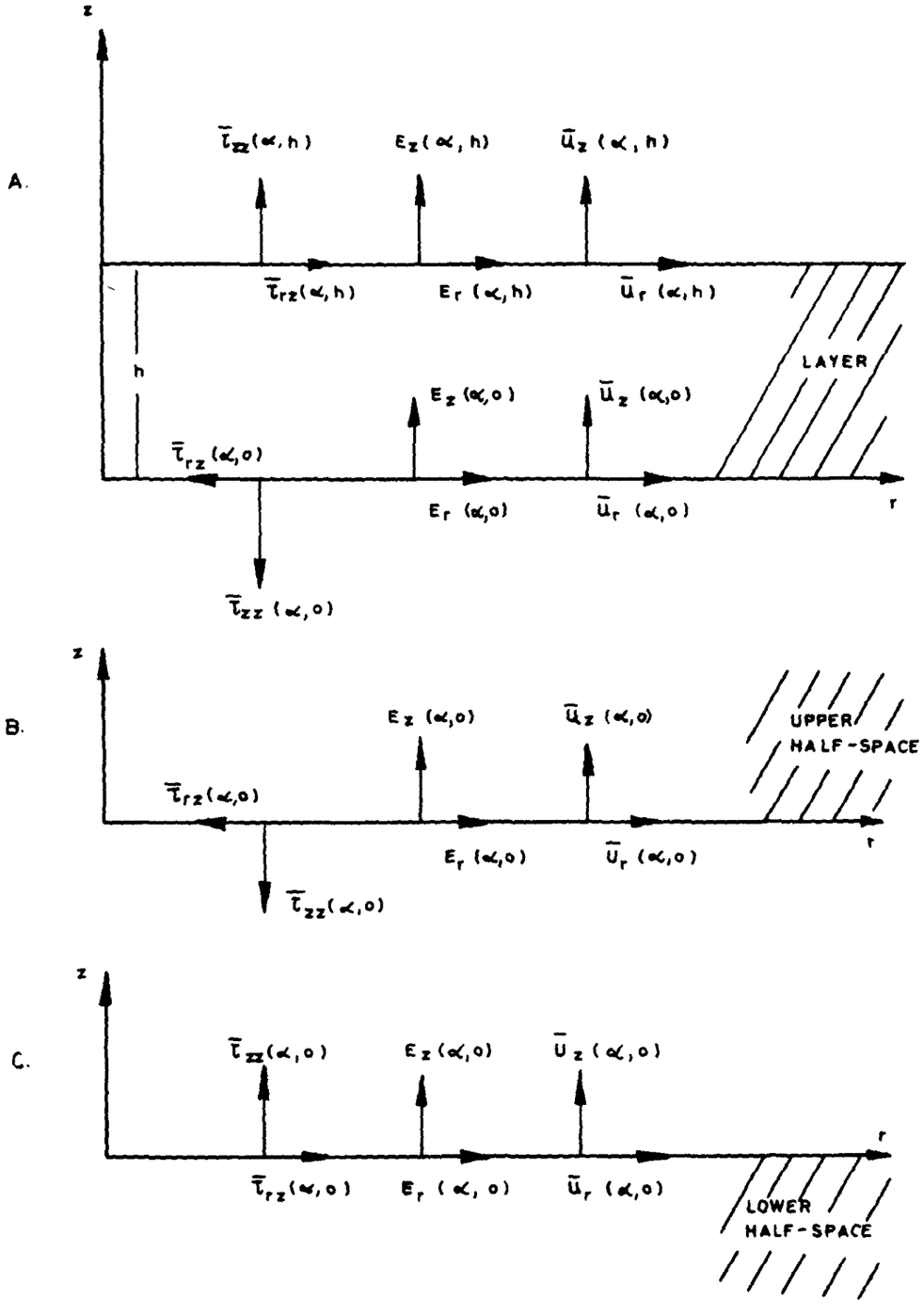

FIG. 3 SPECTRAL STRESSES AND DISPLACEMENTS OF ELASTIC SOLID OR VISCOUS FLUID ELEMENTS

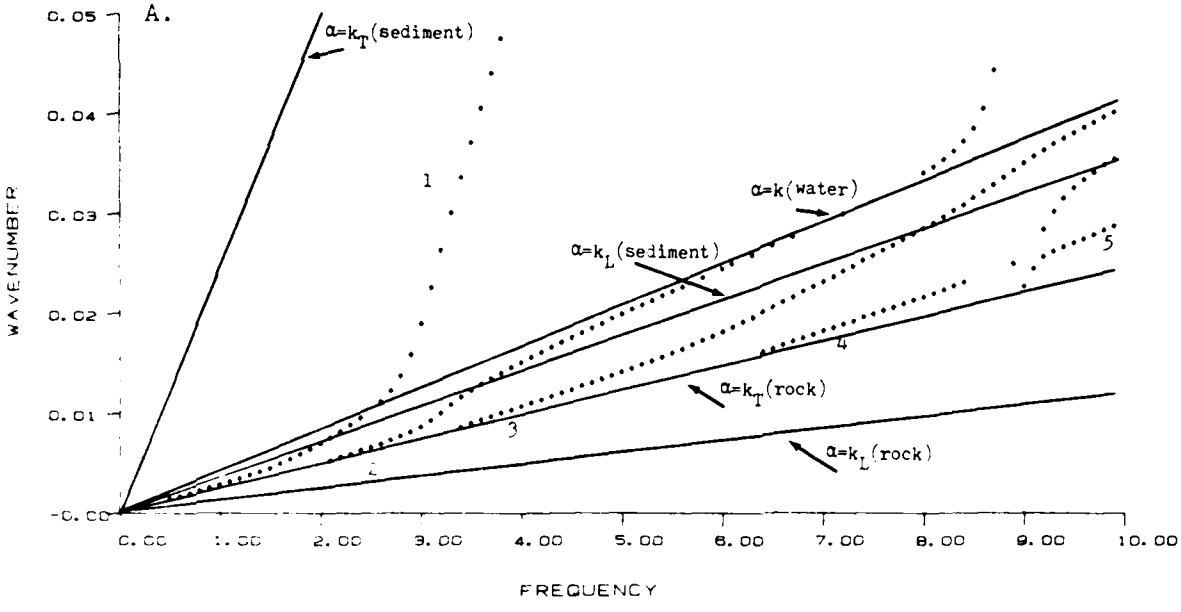

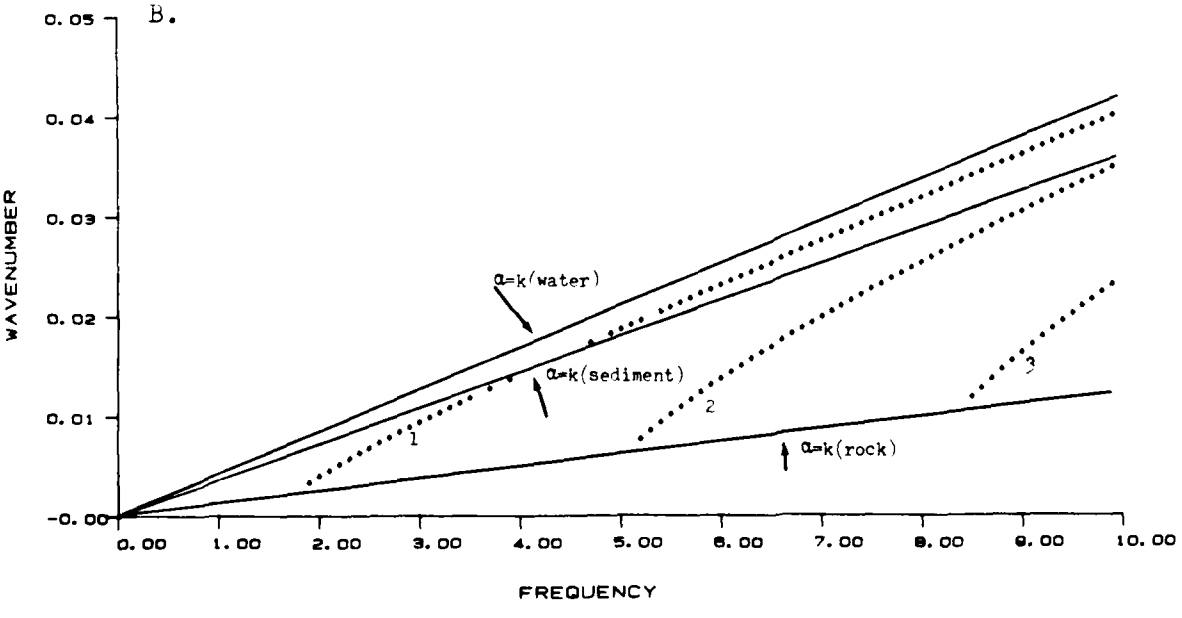

FIG.4 WAVENUMBER VERSUS FREQUENCY PLOTS
(A) WITH SHEAR (B) WITHOUT SHEAR

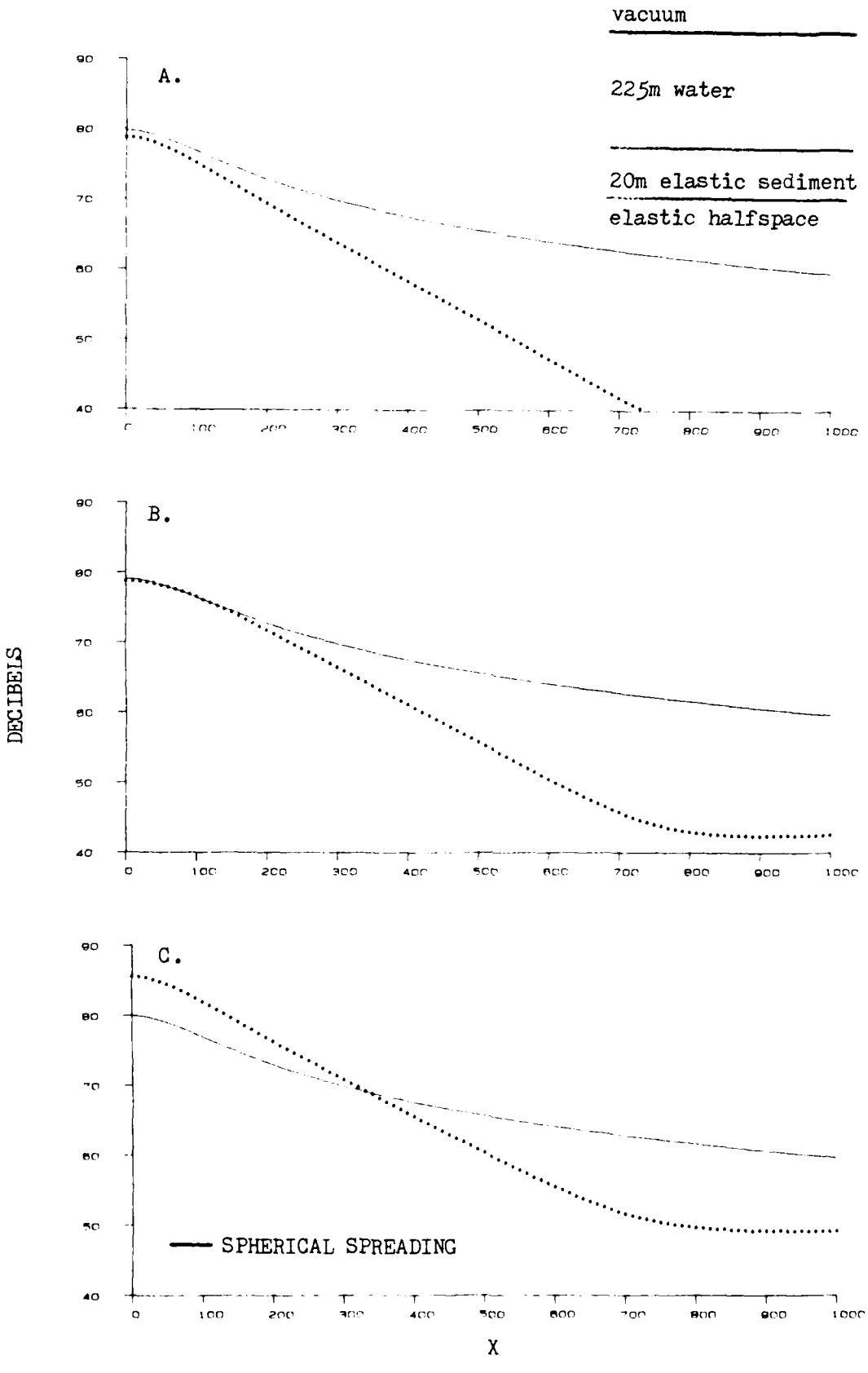

FIG.5 SOUND LEVEL VERSUS DISTANCE (X)
FREQUENCY=1HZ. WITH SHEAR

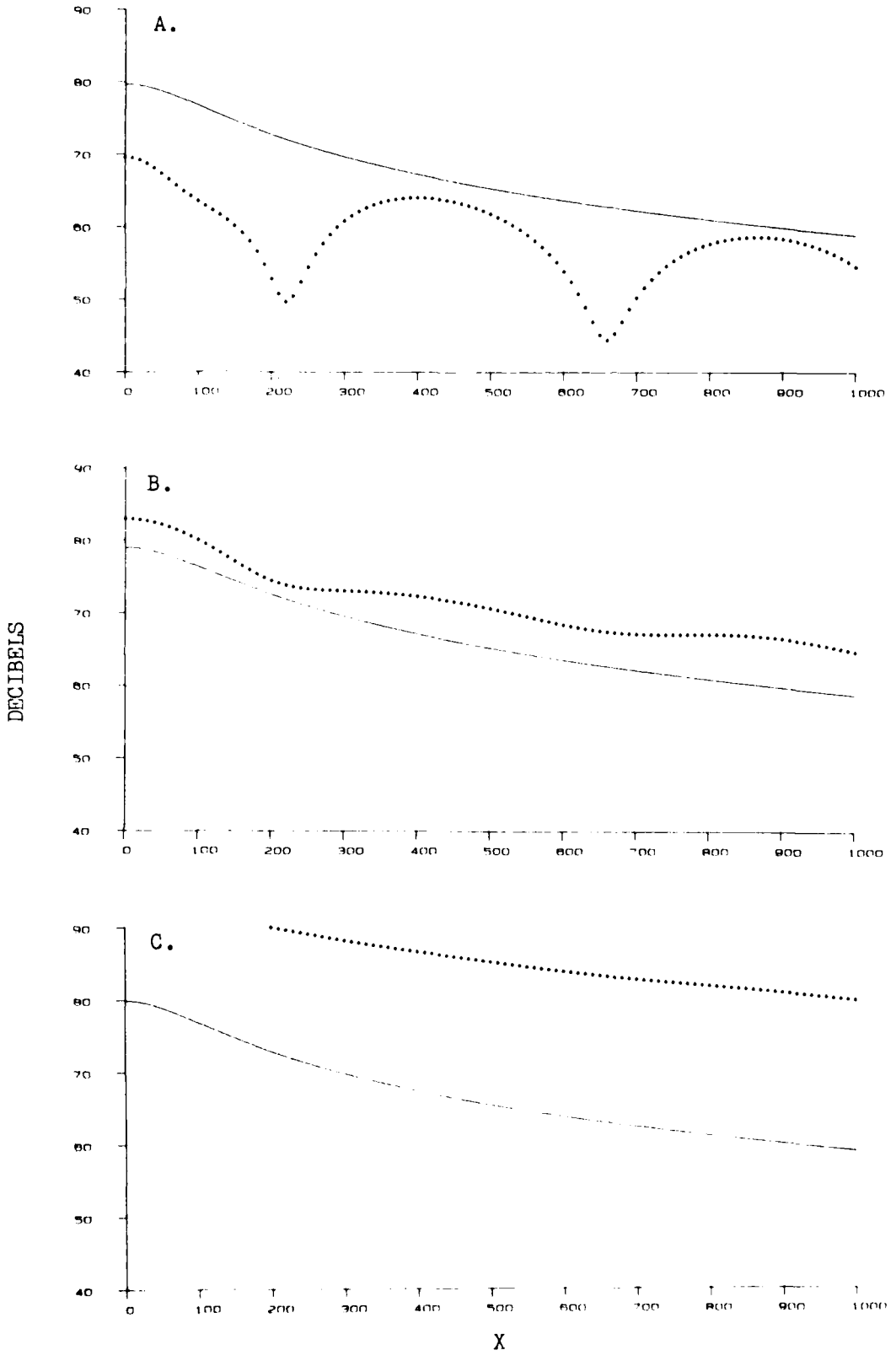

FIG.6 SOUND LEVEL VERSUS DISTANCE (X)
FREQUENCY=3HZ. WITH SHEAR.

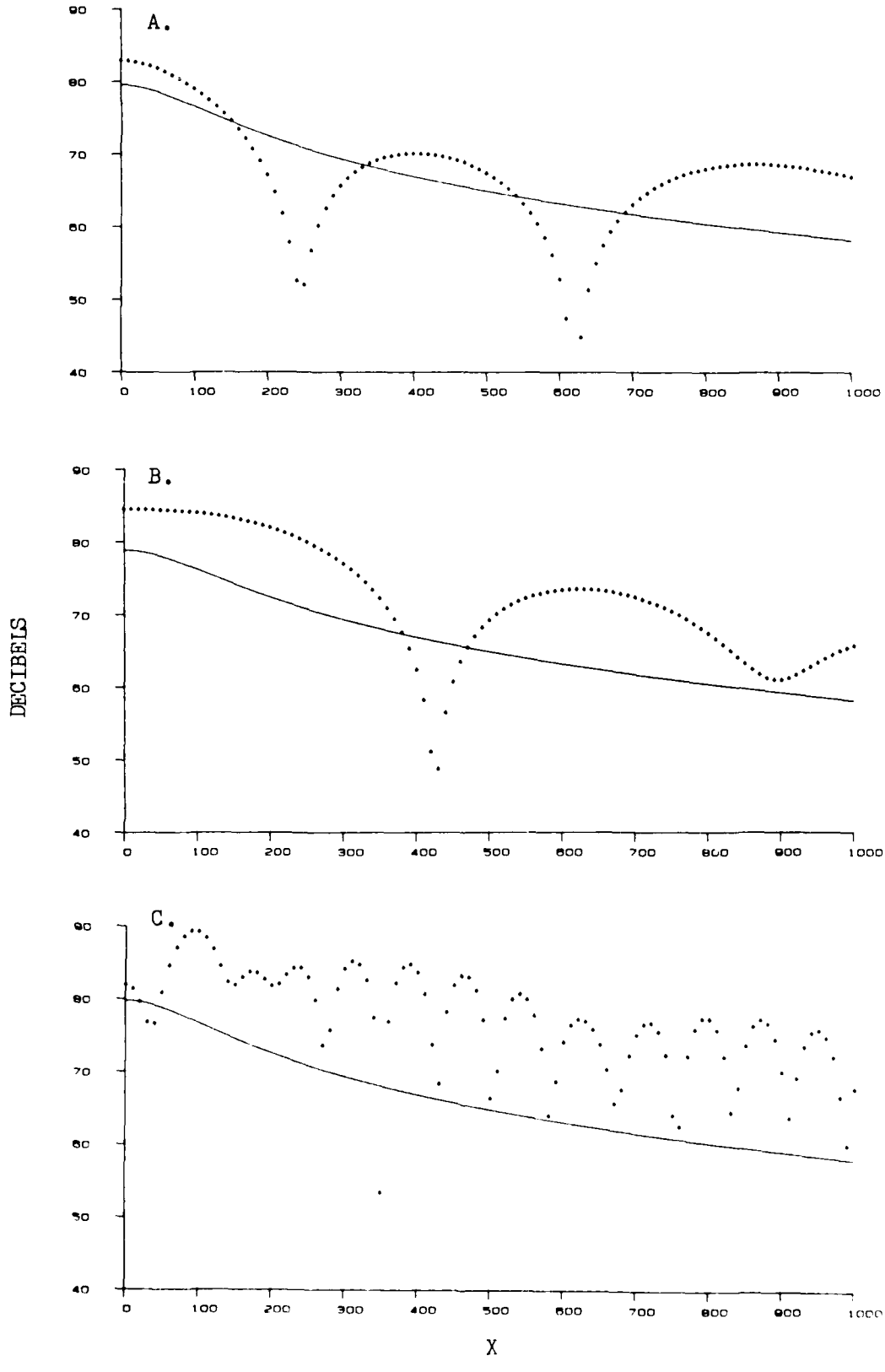

FIG.7 SOUND LEVEL VERSUS DISTANCE (X)
FREQUENCY=5HZ. WITH SHEAR.

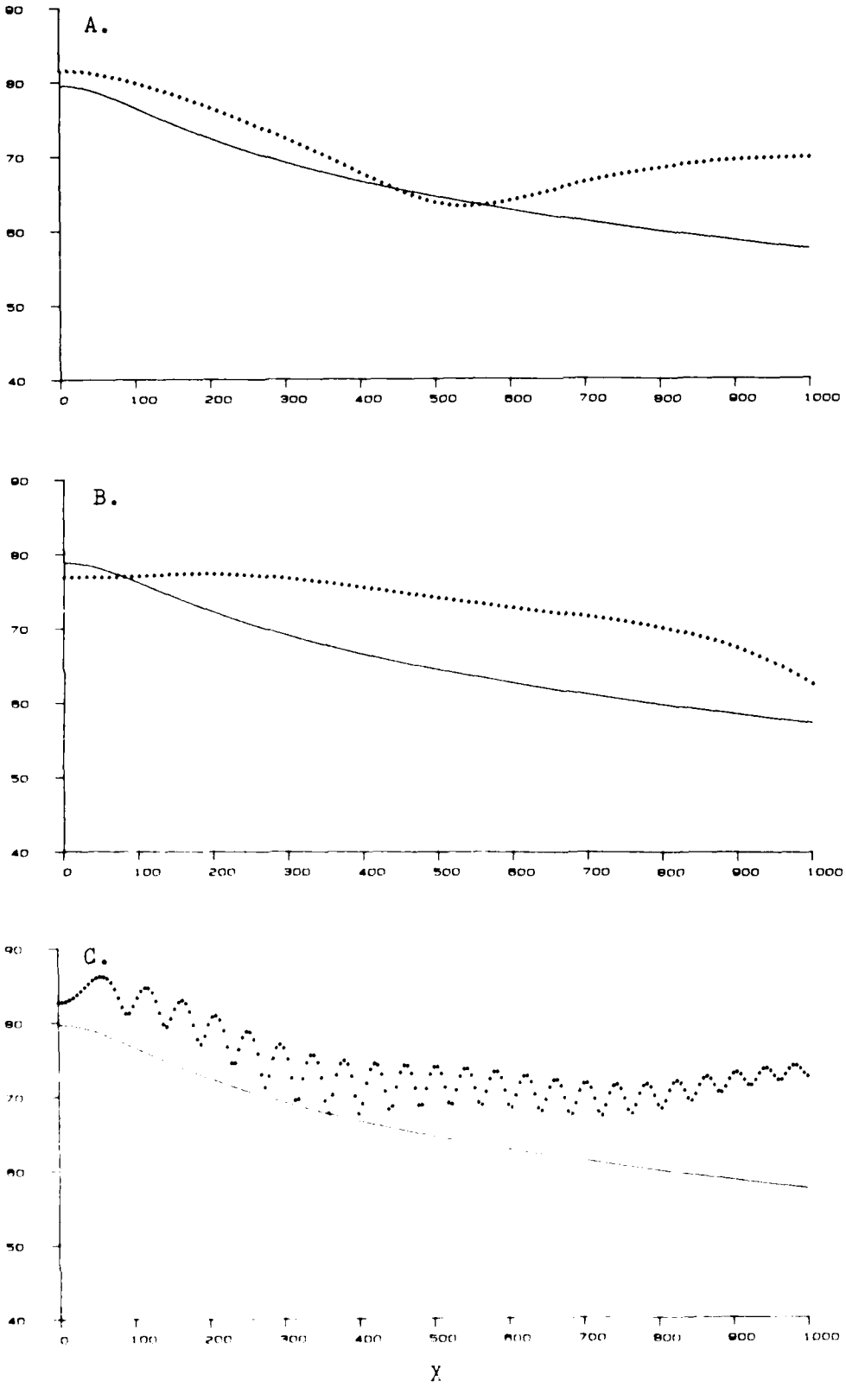

FIG.8 SOUND LEVEL VERSUS DISTANCE (X)
FREQUENCY=7HZ. WITH SHEAR.

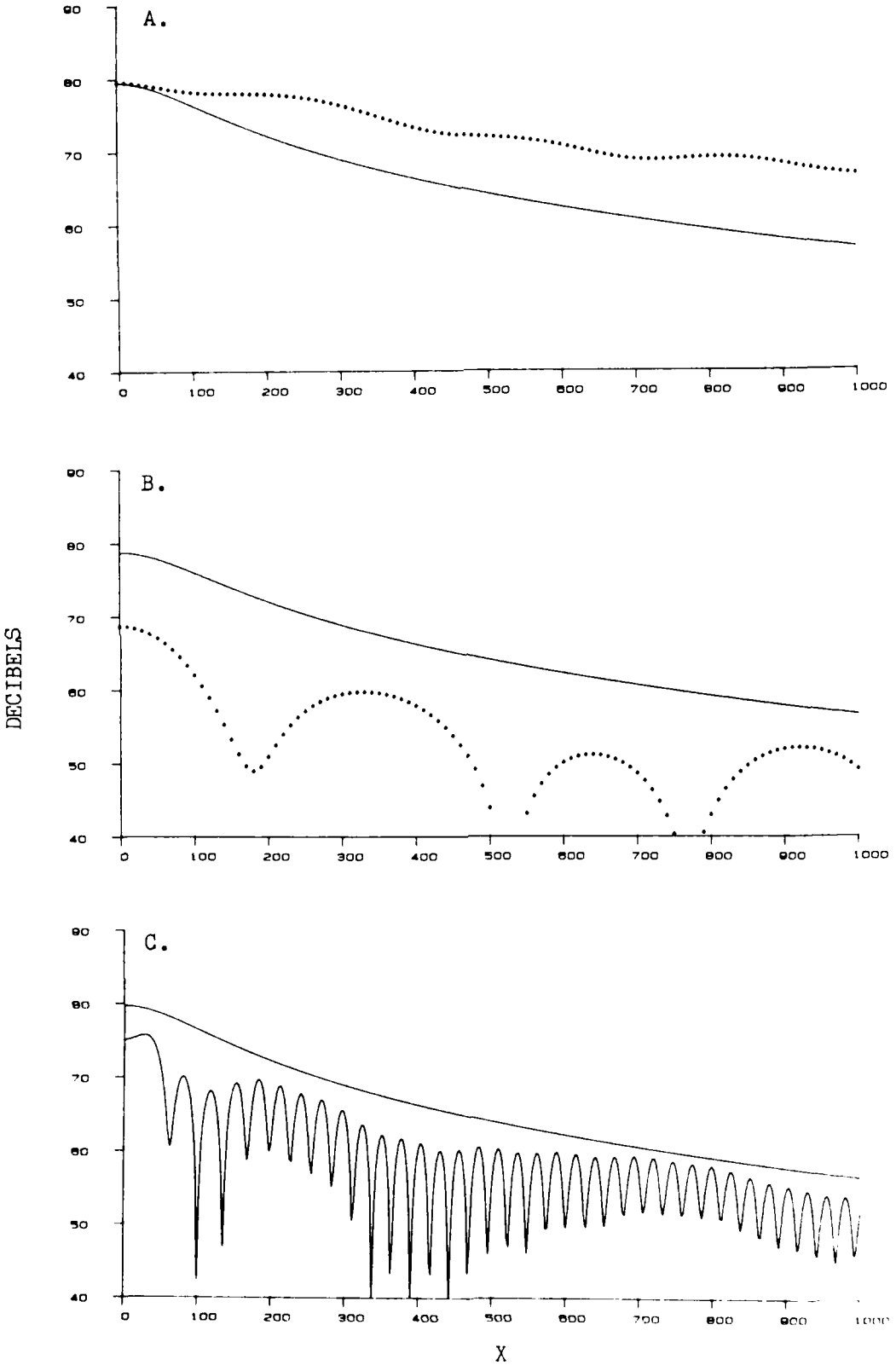

FIG.9 SOUND LEVEL VERSUS DISTANCE (X)
FREQUENCY=9HZ. WITH SHEAR.

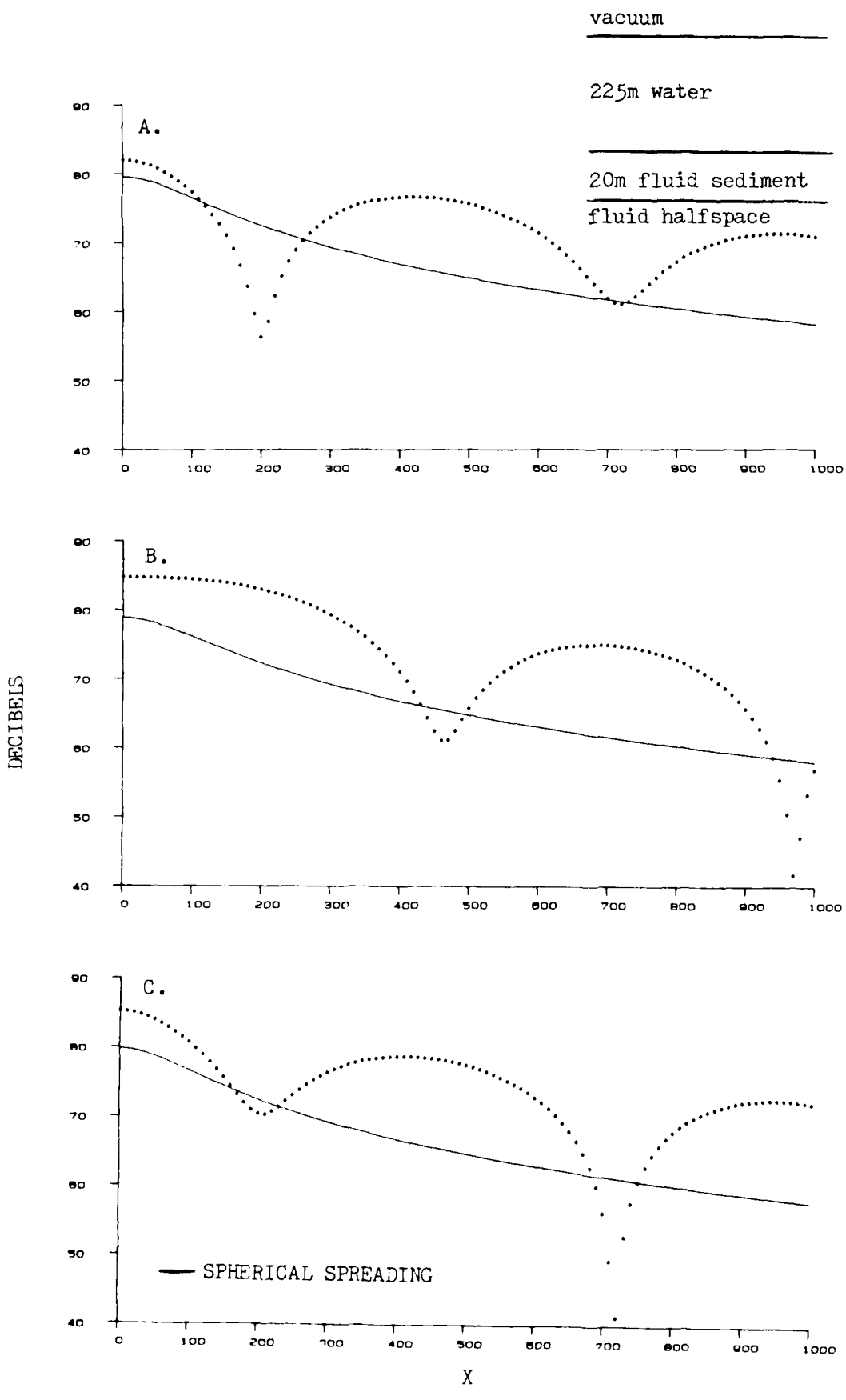

FIG.10 SOUND LEVEL VERSUS DISTANCE (X)
FREQUENCY=5HZ. WITHOUT SHEAR.

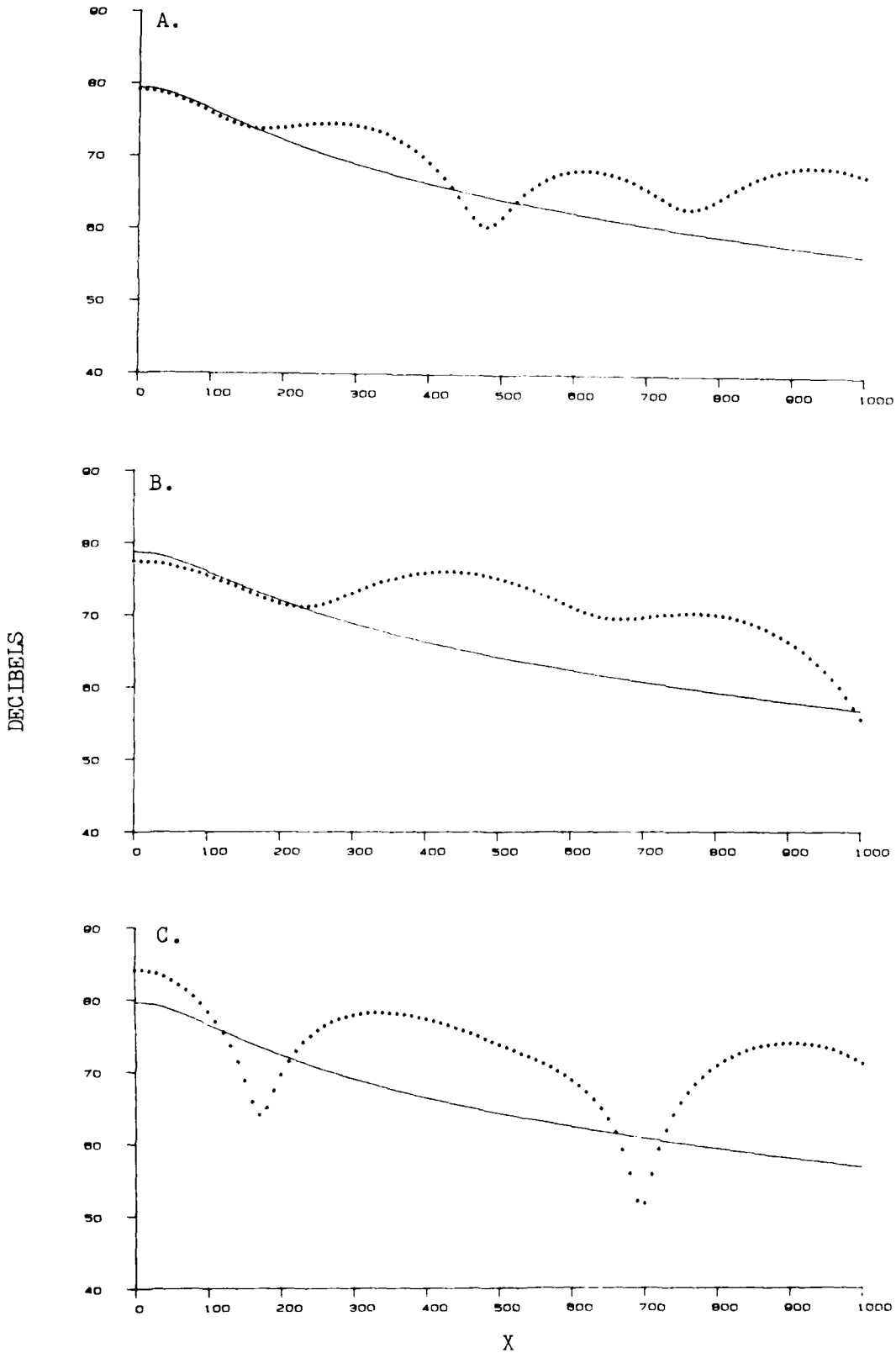

FIG.11 SOUND LEVEL VERSUS DISTANCE (X)
FREQUENCY=9HZ. WITHOUT SHEAR.

A P P E N D I X

The Elastic Layer Matrices $[P_E(\alpha)]$ and $[R_E(\alpha)]$

$$P_{E11} = -2i\mu\alpha\gamma_L \exp(i\gamma_L h) \qquad P_{E12} = 2i\mu\alpha\gamma_L \exp(-i\gamma_L h)$$

$$P_{E13} = \mu\alpha(\gamma_T^2-\alpha^2)\exp(i\gamma_T h) \qquad P_{E14} = \mu\alpha(\gamma_T^2-\alpha^2)\exp(-i\gamma_T h)$$

$$P_{E21} = -(\lambda k_L^2+2\mu\gamma_L^2)\exp(i\gamma_L h) \qquad P_{E22} = -(\lambda k_L^2+2\mu\gamma_L^2)\exp(-i\gamma_L h)$$

$$P_{E23} = 2i\mu\alpha^2\gamma_T \exp(i\gamma_T h) \qquad P_{E24} = -2i\mu\alpha^2\gamma_T \exp(-i\gamma_T h)$$

Rows 3 and 4 are obtained by setting $h=0$ in rows 1 and 2.

$$R_{E11} = -\alpha\exp(i\gamma_L h) \qquad R_{E12} = -\alpha\exp(-i\gamma_L h)$$

$$R_{E13} = -i\alpha\gamma_T \exp(i\gamma_T h) \qquad R_{E14} = i\alpha\gamma_T \exp(-i\gamma_T h)$$

$$R_{E21} = i\gamma_L \exp(i\gamma_L h) \qquad R_{E22} = -i\gamma_L \exp(-i\gamma_L h)$$

$$R_{E23} = \alpha^2 \exp(i\gamma_T h) \qquad R_{E24} = \alpha^2 \exp(-i\gamma_T h)$$

Rows 3 and 4 are obtained by setting $h=0$ in rows 1 and 2.

For the case when $\alpha=0$ the matrix $[R_E(\alpha)]$ is singular and matrix inversion is not possible. However, the non-zero elements of $[\bar{S}_E(0)]$ can be shown to be

$$\bar{S}_{E22} = (\lambda+2\mu)k_L \cos k_L h / \sin k_L h$$

$$\bar{S}_{E24} = -(\lambda+2\mu)k_L / \sin k_L h$$

$$\bar{S}_{E42} = (\lambda+2\mu)k_L / \sin k_L h$$

$$\bar{S}_{E44} = -(\lambda+2\mu)k_L \cos k_L h / \sin k_L h$$

The Elastic Half-space Matrices $[P_E^U(\alpha)]$ and $[R_E^U(\alpha)]$

$$P_{E11}^U = -2i\mu\alpha\gamma_L \qquad P_{E12}^U = \mu\alpha(\gamma_T^2-\alpha^2)$$

$$P_{E21}^U = -(\lambda k_L^2+2\mu\gamma_L^2) \qquad P_{E22}^U = 2i\mu\alpha^2\gamma_T$$

$$R_{E11}^U = -\alpha \qquad R_{E12}^U = -i\alpha\gamma_T$$

$$R_{E21}^U = i\gamma_L \qquad R_{E22}^U = \alpha^2$$

For the case when $\alpha=0$ the matrix $[R_E^U(\alpha)]$ is singular and matrix inversion is not possible. However, the non-zero element of $[\bar{S}_E^U(0)]$ can be shown to be

$$\bar{S}_{E22}^U = i(\lambda+2\mu)k_L$$

The Elastic Half-space Matrices $[P_E^L(\alpha)]$ and $[R_E^L(\alpha)]$

$$P_{E11}^L = 2i\mu\alpha\gamma_L \qquad P_{E12}^L = \mu\alpha(\gamma_T^2-\alpha^2)$$

$$P_{E21}^L = -(\lambda k_L^2+2\mu\gamma_L^2) \qquad P_{E22}^L = -2i\mu\alpha^2\gamma_T$$

$$R_{E11}^L = -\alpha \qquad R_{E12}^L = i\alpha\gamma_T$$

$$R_{E21}^L = -i\gamma_L \qquad R_{E22}^L = \alpha^2$$

For the case when $\alpha=0$ the matrix $[R_E^L(\alpha)]$ is singular and matrix inversion is not possible. However, the non-zero element of $[\bar{S}_E^L(0)]$ can be shown to be

$$\bar{S}_{E22}^L = -i(\lambda+2\mu)k_L$$

.....

END

FILMED

5-85

DTIC